



National
Defence

Défense
nationale



DTIC
ELECTE
JAN 25 1995
C

STUDY OF THE CROSSCORRELATION PROPERTIES OF THE 8-STAGE MAXIMAL LENGTH SEQUENCES FOR THE TESTING OF A TIME-INTEGRATING CORRELATOR (U)

by

S. Faulkner and N. Brousseau

DISTRIBUTION STATEMENT A

Approved for public release.
Distribution Unlimited

19960122 019

DEFENCE RESEARCH ESTABLISHMENT OTTAWA
TECHNICAL NOTE 95-9

Canada

October 1995
Ottawa

DTIC QUALITY INSPECTED 1



National Défense
Defence nationale

STUDY OF THE CROSSCORRELATION PROPERTIES OF THE 8-STAGE MAXIMAL LENGTH SEQUENCES FOR THE TESTING OF A TIME-INTEGRATING CORRELATOR (U)

by

S. Faulkner and N. Brousseau
Electronic Support Measures Section
Electronic Warfare

Accession For	
NTIS ORAD	<input checked="" type="checkbox"/>
DTIC TAB	<input type="checkbox"/>
Unannounced	<input type="checkbox"/>
Justification	
By	
Distribution/	
Availability Codes	
Dist	Avail and/or Special
A-1	

DEFENCE RESEARCH ESTABLISHMENT OTTAWA
TECHNICAL NOTE 95-9

PCN
02J01

October 1995
Ottawa

ABSTRACT

The purpose of this DREO Technical Note is to present experimental and theoretical results on the properties of the crosscorrelations of maximum length direct sequences (m-sequences). The code correlation families and the relationship between full-period and partial-period correlations are described. Results from the software developed to study the crosscorrelation properties of the 8-stage m-sequences, denoted R8's, as well as results obtained from the optical correlator and the theoretical studies are presented. The software developed to analyze the crosscorrelation functions was also suitable for the study of partial-period correlation functions and the study of the effects of phase shifts on partial-period correlation functions. Properties of partial-period correlation functions are also analyzed and a generalization to longer m-sequences is presented. The results from the optical correlator demonstrate that it is possible to visually identify the m-sequence family associated with the crosscorrelations for those which have the strongest features.

RÉSUMÉ

Cette note technique de CRDO présente des résultats expérimentaux et théoriques sur les propriétés des intercorrélations de séquences directes à longueur maximale (séquence-m). On y décrit les familles de corrélation de codes et les liens entre les corrélations à période partielle et à période entière. On présente également des résultats provenant de logiciels conçus pour étudier les propriétés des intercorrélations de séquences-m à 8 stages (R8), des résultats produits par un corrélateur optique et des résultats théoriques. Les logiciels conçus pour l'analyse des fonctions d'intercorrélations sont aussi utilisables pour l'analyse des fonctions de corrélation à période partielle. On analyse les propriétés des corrélations à périodes partielles et on généralise les résultats pour des séquences-m plus longues. Les résultats du corrélateur optique démontrent qu'il est possible d'identifier visuellement les familles de séquences-m associées aux intercorrélations ayant les caractéristiques les plus accusées.

EXECUTIVE SUMMARY

One of the objectives of the Future Multi-Environment Electronic Warfare Thrust is to exploit new developments in signal processing.

Code Division Multiple Access (CDMA) mobile communications is now used by terrestrial cellular telephone systems and has been proposed for satellite cellular communication systems. The crosscorrelation properties of the spreading codes used for CDMA communications have an important impact on their performance.

The purpose of this DREO Technical Note is to present a theoretical study of the crosscorrelation properties of the R8's and to apply these results to the testing of an optical correlator. The operation and the main feature of the optical correlator are described and the software developed to study the crosscorrelation properties of the R8's is presented. The theoretical background on the crosscorrelation of the R8's is then reviewed and their most important properties are noted. The properties of partial-period correlation functions are then analysed and a generalization to longer m-sequences is presented. A time-integrating correlator (TIC) is then used to produce experimental results that are compared to the theoretical results. The identification of the m-sequence family associated with the crosscorrelations is possible for those which have the strongest features.

TABLE OF CONTENTS

	<u>PAGE</u>
ABSTRACT/RESUME	iii
EXECUTIVE SUMMARY	v
TABLE OF CONTENTS	vii
LIST OF FIGURES	ix
LIST OF TABLES	xi
1.0 INTRODUCTION	1
2.0 TIME-INTEGRATING CORRELATOR	4
3.0 R8 SIMULATION	12
4.0 ANALYSIS OF R8 CROSSCORRELATION PROPERTIES	15
4.1 Partial-Period Crosscorrelation Properties for the R8's	20
5.0 EXPERIMENTAL RESULTS	32
6.0 CONCLUSION	33
7.0 REFERENCES	33

LIST OF FIGURES

	<u>PAGE</u>
FIGURE 1: SPREAD SPECTRUM SIGNAL	2
FIGURE 2: MODES OF OPERATION OF A CORRELATOR	3
FIGURE 3: TIME-INTEGRATING CORRELATOR SCHEMATIC	5
FIGURE 4: TIME-INTEGRATING CORRELATOR	6
FIGURE 5: CORRELATION PROCESS IN A TIC	8
FIGURE 6: AUTOCORRELATION SIGNALS FROM A TIC	9
FIGURE 7: PEDESTAL SUBTRACTION PROCESS	11
FIGURE 8: DECIMATION RELATIONS FOR THE R5'S (FROM [5])	17
FIGURE 9: DECIMATION RELATIONS FOR THE R8'S (FROM [5])	18
FIGURE 10: CODE FAMILIES FOR THE R8'S (FROM [5])	19
FIGURE 11: CROSSCORRELATION FUNCTIONS FOR THE R8'S (FROM [5]) (1)	21
FIGURE 12: CROSSCORRELATION FUNCTIONS FOR THE R8'S (FROM [5]) (2)	22
FIGURE 13: CROSSCORRELATION FUNCTIONS FOR THE R8'S (FROM [5]) (3)	23
FIGURE 14: CROSSCORRELATION FUNCTIONS FOR CODES 0 AND 5	24
FIGURE 15: VARIATION IN PEAK AMPLITUDES FOR THE PARTIAL-PERIOD CROSSCORRELATION BETWEEN CODES 0 AND 5; PEAK 1 AT 95, INTEGRATION OF 250, 230 AND 210 CHIPS	26
FIGURE 16: VARIATION IN PEAK AMPLITUDES FOR THE PARTIAL-PERIOD CROSSCORRELATION BETWEEN CODES 0 AND 5; PEAK 2 AT 63, INTEGRATION OF 250, 230 AND 210 CHIPS	27
FIGURE 17: VARIATION IN PEAK AMPLITUDES FOR THE PARTIAL-PERIOD CROSSCORRELATION BETWEEN CODES 0 AND 5; PEAK 3 AT 95, INTEGRATION OF 250, 230 AND 210 CHIPS	28
FIGURE 18: OPTICALLY PRODUCED CROSSCORRELATIONS FUNCTIONS FOR THE R8'S (1)	29
FIGURE 19: OPTICALLY PRODUCED CROSSCORRELATIONS FUNCTIONS FOR THE R8'S (2)	30
FIGURE 20: OPTICALLY PRODUCED CROSSCORRELATIONS FUNCTIONS FOR THE R8'S (3)	31

LIST OF TABLES

	<u>PAGE</u>
TABLE 1: SEQUENCE GENERATOR FEEDBACK TAPS FOR THE R8'S	11
TABLE 2: MEAN AND VARIANCE OF THE THREE HIGHEST PEAKS OF THE PARTIAL-PERIOD CROSSCORRELATION FUNCTION BETWEEN CODES 0 AND 5 FOR DIFFERENT INTEGRATION TIME WINDOWS	25
TABLE 3: FEATURES OF THE CROSSCORRELATION FUNCTIONS FOR THE R8'S	32

1.0 INTRODUCTION

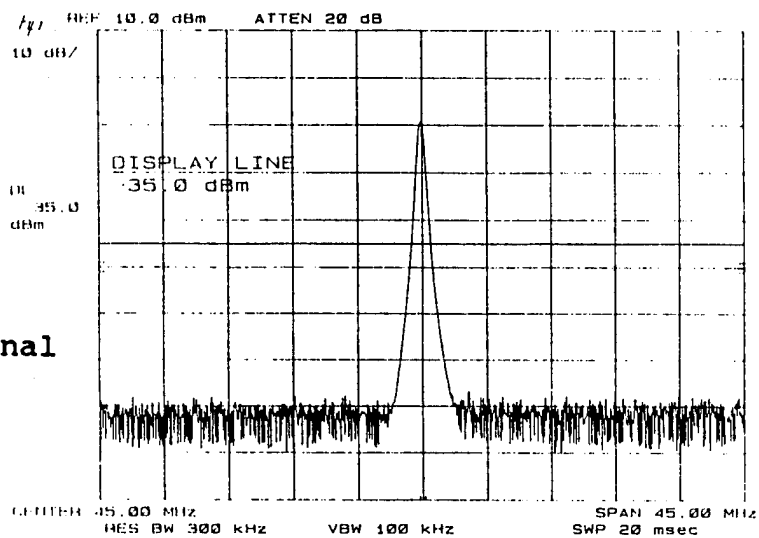
Direct sequences techniques are being utilized in modern military communication systems due to their inherent resistance to jamming and interception [1]. In particular, the utilization of direct sequences to achieve the spectral spreading of the signal can lead to situations where the presence of a communication signal is very difficult to detect with conventional spectral analysis. Figure 1a illustrates the spectrum of a voice signal with a narrow bandwidth of 25 kHz. The spread version of the signal is illustrated in Figure 1b where the spectrum has been expanded by multiplying the data by a high rate spreading code. The expansion factor, or processing gain, typically ranges from 100 to 10,000. Since the total power of the signal stays the same, the power spectral density of the spread signal is much lower. The existence of noise may make the detection of signals such as they are illustrated in Figure 1c very difficult.

However, it is possible to detect spread spectrum signals buried in noise with specialized processing such as correlation. Correlation is a comparison process which permits detection of the presence of signals buried in noise. In many cases, correlation will even permit detection of signals which would be undetectable by spectral analysis. In a first mode of operation (see Figure 2a), the detection mode, the signals received by two different antennas are processed by the correlator. If there is a common element in the two signals being compared, a characteristic correlation peak will appear, indicating the presence of signal in the noisy background. Experimental results [1] have demonstrated that it is possible to detect a correlation peak when both input signals are as low as -24 dB relative to the noise.

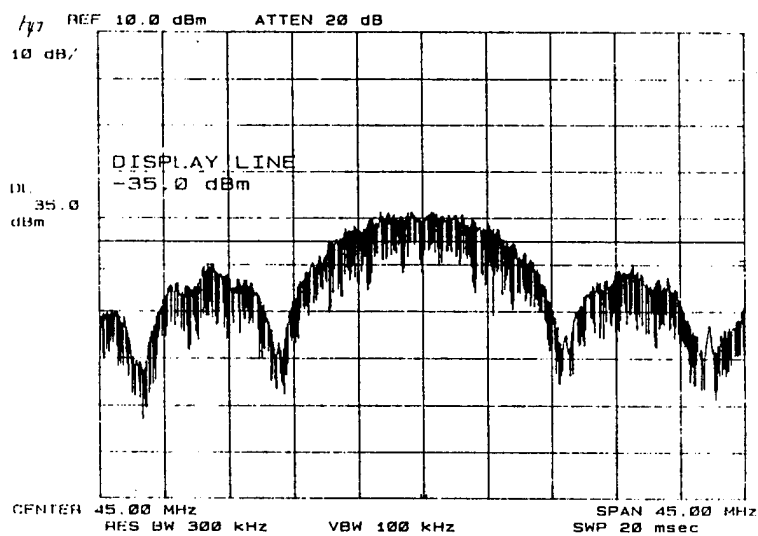
In a second mode of operation (see Figure 2b), the matched filter mode, the signal received by one antenna is applied to one of the input ports of the correlator while a reference signal is applied to the second port. The presence of a strong correlation peak indicates that the reference signal and the unknown signal are identical. Detectable correlation peaks have been observed [1] with a reference signal at 0 dB and the unknown signal at -43 dB relative to the noise.

DREO is involved in the development of a prototype of a Time-Integrating Correlator (TIC) using acousto-optic technology. A digital post-processor controls the flow of input and output data to the TIC. It is planned to evaluate the prototype system by using the auto and crosscorrelation functions produced by short maximum-length sequences of period 255 chips, termed the R8's. The term R8 refers to a maximum-length sequence, or m-sequence, generated by an eight-stage shift register generator. R8 sequences contains $2^8 - 1 = 255$ chips.

a)
narrowband signal



b)
after spreading



c)
spread spectrum
signal in noise

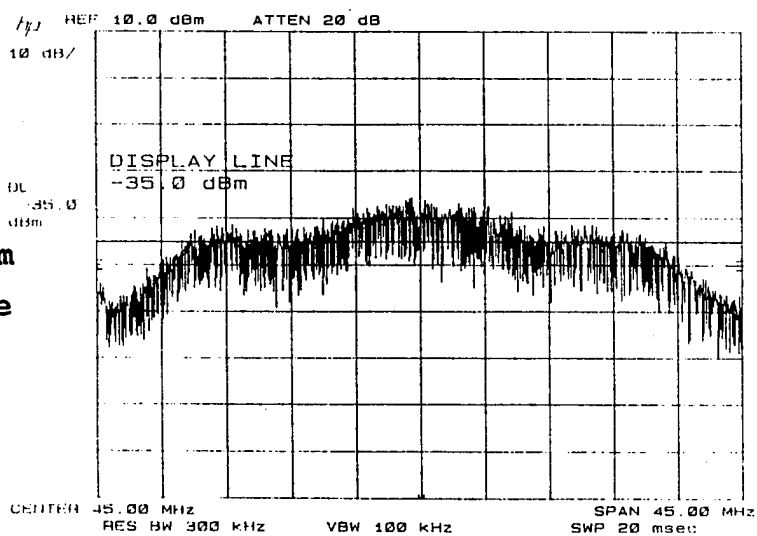
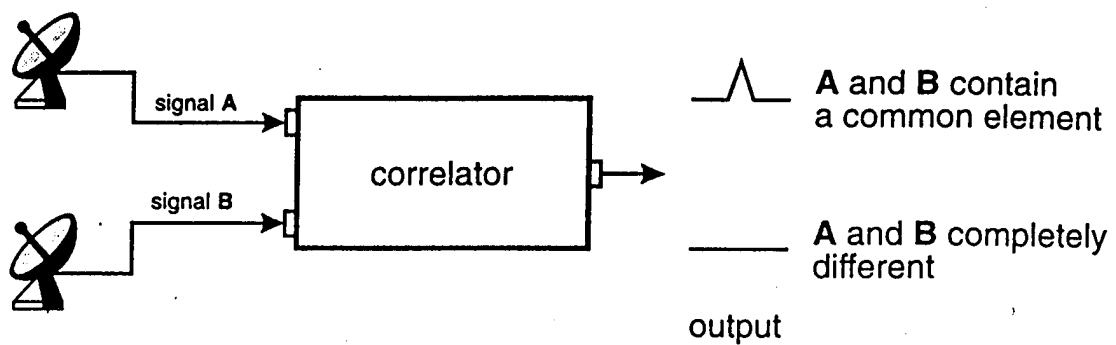
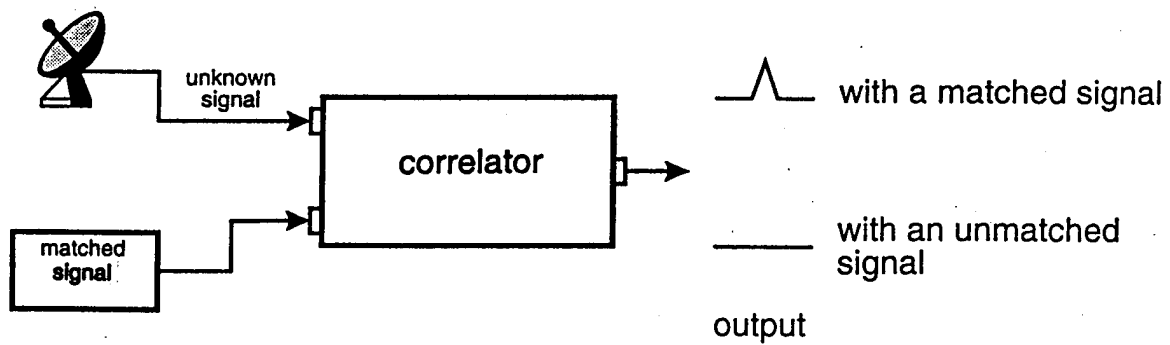


FIGURE 1: SPREAD SPECTRUM SIGNAL



a)



b)

FIGURE 2: MODES OF OPERATION OF A CORRELATOR
 (a) DETECTION
 (b) MATCHED FILTER

There are 16 different R8 sequences with 16 possible full-period autocorrelation functions. A full period autocorrelation function is produced when the autocorrelation is calculated for all the chips of the sequence with an integration time equal to the duration (or to an integer multiple of the duration) of a sequence. The number of full-period crosscorrelation patterns is 240 because they are formed by two different sequences. There are 16 possible choices for the first sequence and only 15 choices are left for the second one. A study of the crosscorrelation properties of the R8's was undertaken in order to identify pairs of sequences whose crosscorrelation function exhibits special characteristics that are relevant to the testing of a correlator.

The purpose of this Technical Note is to present the crosscorrelation properties of the R8's and to compare some of the theoretical results as obtained from a computer simulation with the experimental results as obtained from an optical correlator. The software developed to analyze the crosscorrelation functions was also suitable for the study of partial-period correlation functions. A partial period correlation is produced when the correlation is calculated for all the chips of the sequences with an integration time that is not equal to the duration (or to an integer multiple of the duration) of a sequence. The partial period correlation depends on which chip each sequence starts. The position of the initial chip in a sequence relative to some reference starting point is called the phase of the sequence. Properties of partial-period correlation functions are also analyzed and a generalization to longer m-sequences is presented. A brief description of the operation of the TIC and its post-processor is now presented.

2.0 TIME-INTEGRATING CORRELATOR (TIC)

The TIC developed at DREO is an optical system using acousto-optic interaction producing the correlation of two signals without having to time invert either of them. The correlator uses a tandem configuration where the two laser beams interact with the Bragg cells and propagate on an almost common path (see Figure 3 and Figure 4). The light from a laser is expanded, then split into two paths by the holographic beam-splitter. Each of the two beams interact with only one of the Bragg cells A and B. The RF signals produced either by two antennas or by one antenna and a signal generator are applied to the transducers of the Bragg cells. The transducers transform the electromagnetic waves into acoustic waves propagating in the transparent crystal of the Bragg cell. The propagating acoustic waves act like moving diffraction gratings and diffract some of the incident light. The information carried by the RF signal is thus transferred to the two diffracted light beams that are imaged by a lens on a photodetector in such a way that the waves are counterpropagating. Each element of the photodetector performs a time integration of the incident signals.

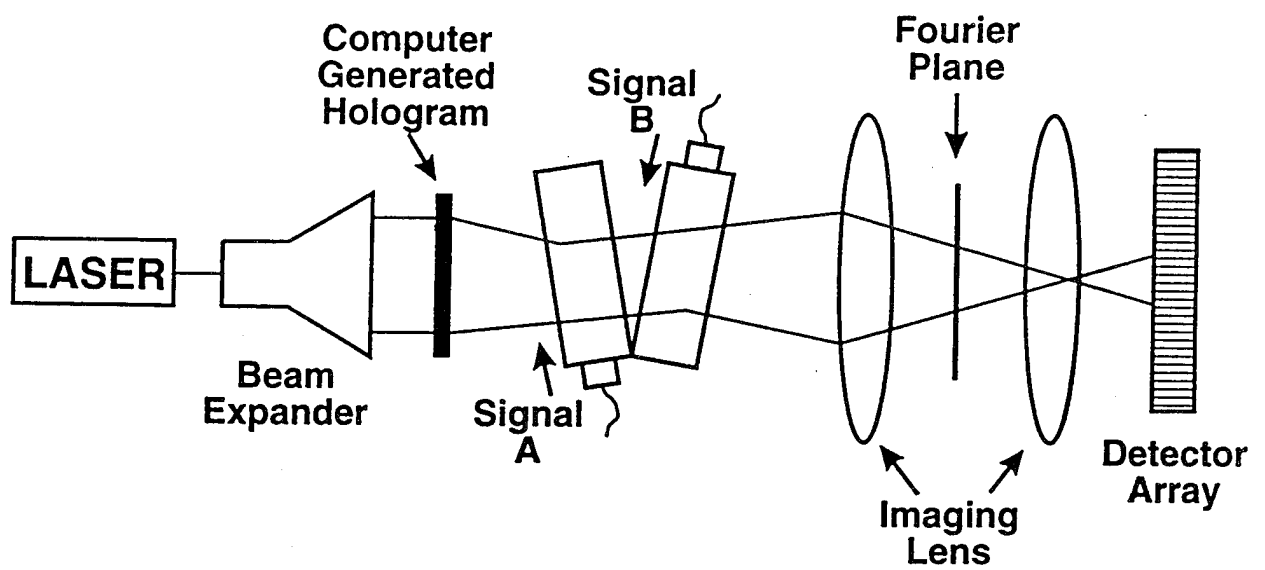


FIGURE 3: TIME-INTEGRATING CORRELATOR SCHEMATIC

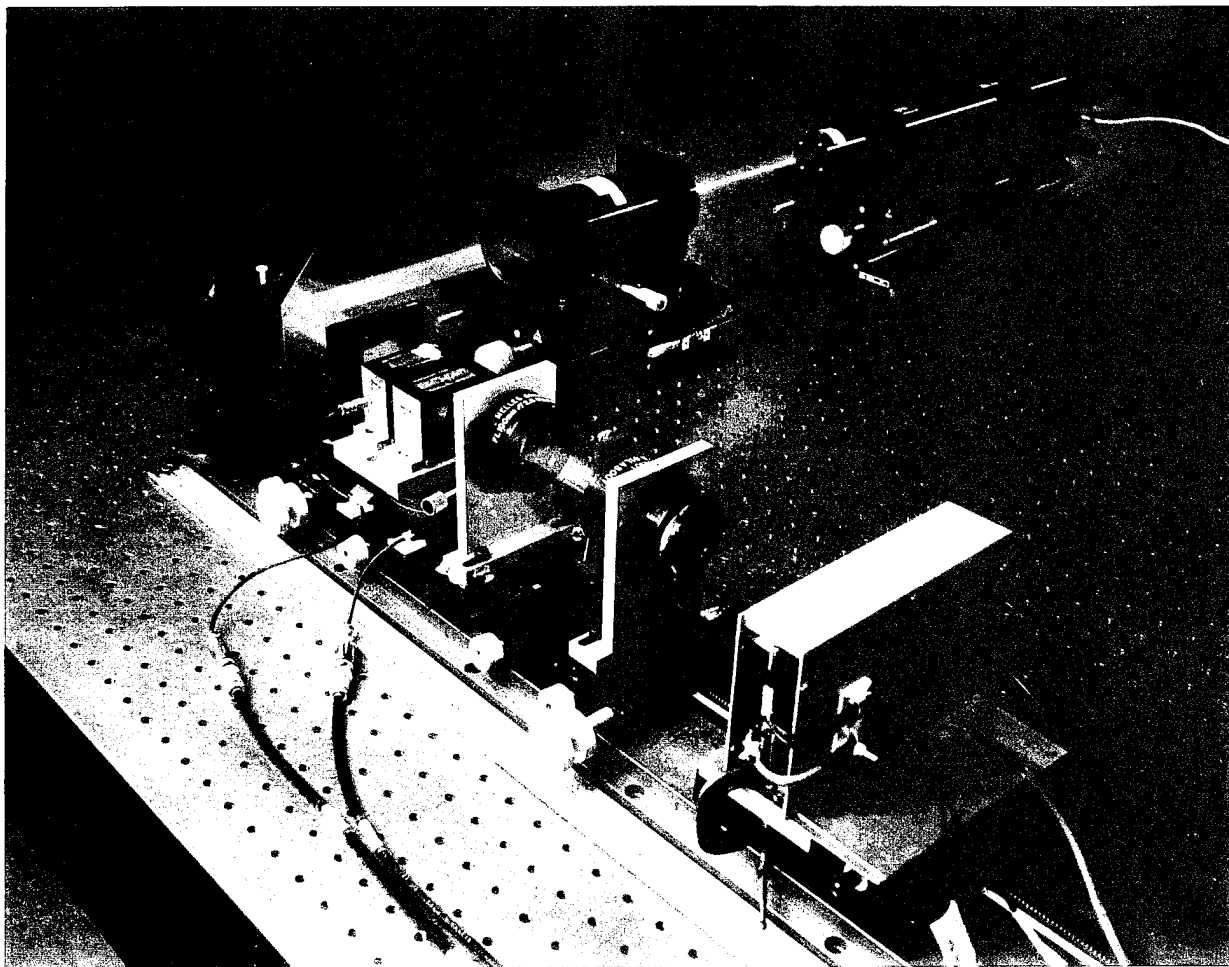


FIGURE 4: TIME-INTEGRATING CORRELATOR

The correlation process is illustrated in Figure 5 using two simple identical counterpropagating waveforms A and B and three elements of a detector array. In the first column of Figure 5, the successive positions of the two counterpropagating signals are illustrated for five different time intervals. In the second column, the products $A \times B$ of the two signals are illustrated and the third column shows the results of the time integration performed by the elements of the array. At time $t=t_0$, illustrated on the first row, the two counterpropagating signals are not yet superimposed, the product $A \times B$ is still null and no energy has been collected by the three detecting elements. In the second row, at time $t=t_1$, the signals A and B are partially overlapping. However, their product does not yet exist on detectors 1 and 3 and only detector 2 has integrated some energy. At time $t=t_2$, illustrated in the third row, the two signals have propagated further and now the product of $A \times B$ also exists on detectors 1 and 3 and they start to accumulate energy. At time $t=t_3$, the signals completely overlap and the product $A \times B$ is at its widest. All three detector elements are integrating energy at that moment. The last row illustrates the situation at $t=t_4$ when the two signals have propagated even further, and are about to stop overlapping. Only detector number 2 is still collecting energy at that moment and the correlation peak produced by the energy build-up on the three detector elements can be observed.

A simplified expression for the correlation function $I(z, t)$ produced by the TIC is described by the equation:

$$\begin{aligned}
 I(z, t) = & \int^T A^2(t+z/v) dt \\
 & + \int^T B^2(t-z/v) dt \\
 & + \int^T 2A(t+z/v) B^*(t-z/v) dt
 \end{aligned} \tag{1}$$

where $A(t)$ and $B(t)$ are the two signals to be correlated, v is the acoustic propagation velocity, and z is the distance along the Bragg cell (the position of the center of the Bragg cell is $z=0$). The first two terms, the integrals of $A^2(t)$ and $B^2(t)$, contribute to the formation of a pedestal (see Figure 5 at $t=t_4$) over which the correlation term appears. The integration performed by the detector array over a time T produces a third term that can be recognized as the correlation of the two input signals.

A typical correlation pattern produced by an acousto-optic TIC is illustrated in Figure 6. The shape of the autocorrelation peak contains information about the input signals. The width of the base of the triangular envelope of the peak is equal to the time width of a chip from the sequence being correlated. The position of the peak depends on the difference of time of arrival

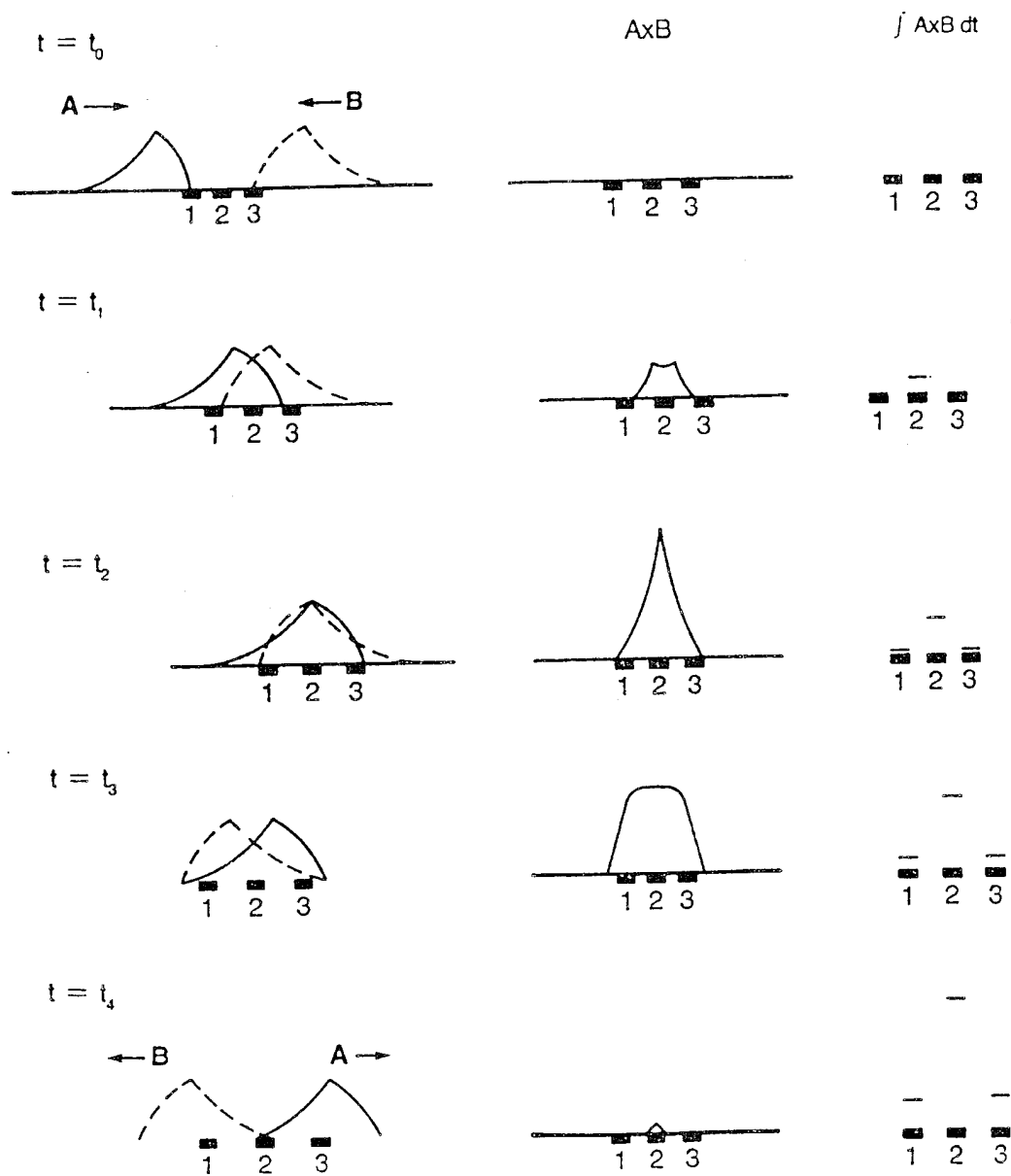


FIGURE 5: CORRELATION PROCESS IN A TIC

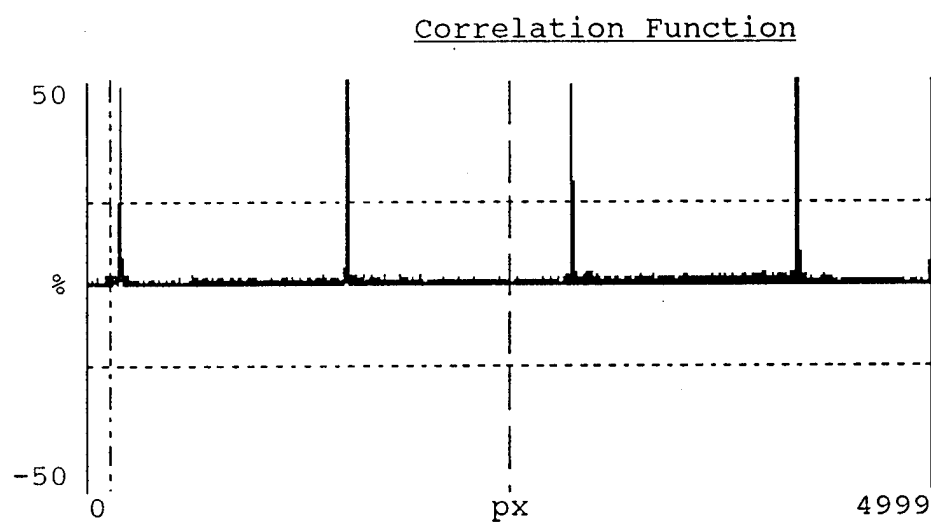


FIGURE 6 : AUTOCORRELATION SIGNALS FROM A TIC

of the two signals and can provide information on direction of arrival. The position of the marker set by the user is given in number of elements of the detector array called pixels or "px" on Figure 6. Although not visible on Figure 6, the modulation of the peak by an optimal fringe system [2] allows one to maintain the height of the peak above a minimum for all positions of the peak relative to the detector array.

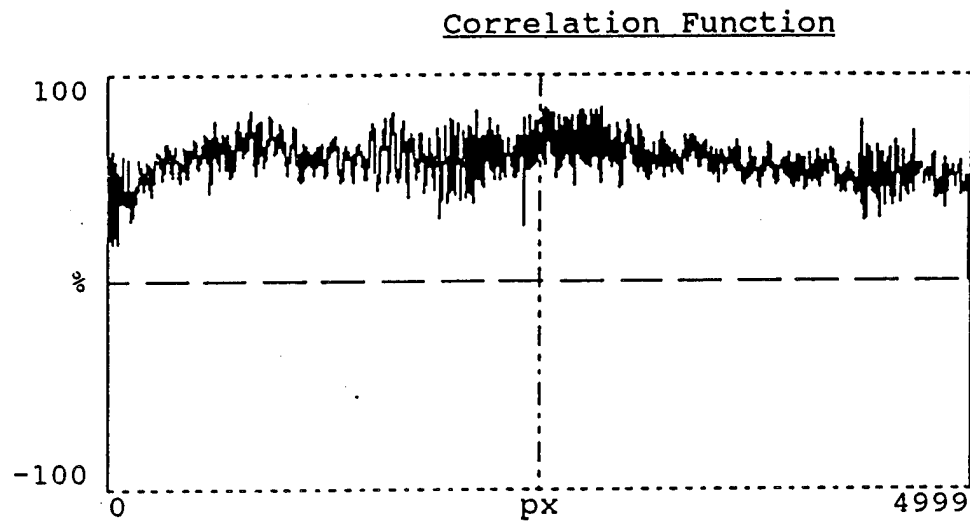
The correlation peak appears over a pedestal which is generated by the first two terms of Eq. 1. However, it is possible to remove the pedestal by subtracting from the last collected correlogram, a previously recorded correlogram (used as a reference and illustrated on Figure 7a) which does not contain a correlation peak. The pedestal is thus removed and the peak is left intact (see Figure 7b). The reference is updated after a set time. The operations required to perform the pedestal removal are under the control of the post-processor. The post-processor also allows the operator to specify operating parameters such as the integration time, or the spreading of the signals. From the parameters specified by the operator, the post-processor controls the flow of input and output data to the TIC. The post-processor also includes software to perform peak detection and to analyze the features of the peak.

The TIC built at DREO includes two TeO_2 Bragg cells (see Figure 7) with a bandwidth of 30 MHz centered at 45 MHz. The transit time of the acoustic signal in the Bragg cell is 40 μs . When the TIC is operated in the detection mode, it is thus possible to correlate two signals with up to 80 μs of difference between their times of arrival. The position of the correlation peak then depends on the difference of the times of arrival of the two signals at the receiving antenna. The time integration is performed by a Kodak linear detector array having five thousand 7 μm by 7 μm elements. It is possible to control the integration time with the post-processor.

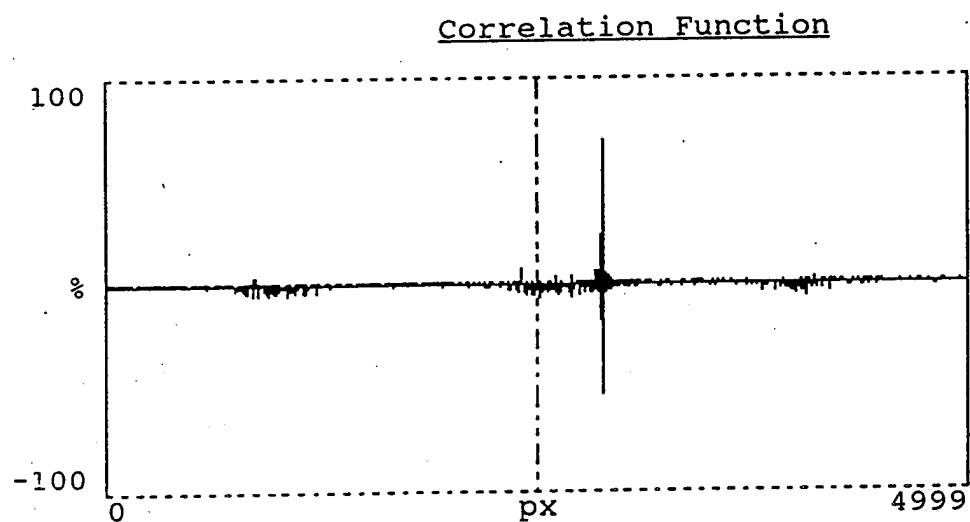
Thorough testing and performance analysis of the system it is required to use a set of experiments with known results. It was decided to use the R8's for testing purposes. There are 16 R8's (eight sequences and their reverses) so 240 full-period crosscorrelation patterns are possible. The taps used to generate the sequences [2] are listed in Table 1. The notation 4,3,2 for code 0 corresponds to the R8 with characteristic polynomial $g(x) = x^8 + x^4 + x^3 + x^2 + 1$. Alternately, the polynomial $g(x)$ can be expressed in octal notation. The above polynomial is represented by the binary vector 100011101 which is expressed as 435 in octal notation. The decimation notation will be explained in Section 4.0. The R8's are a set of sequences which are sufficiently small to permit the calculation of all full-period crosscorrelation patterns and to permit the selection of a few that are most appropriate for the testing of the TIC.

TABLE 1: SEQUENCE GENERATOR FEEDBACK TAPS FOR THE R8'S

Code ID	Polynomial Taps	Decimation	Octal Representation
0	4,3,2	1	435
1	6,5,3	7	551
2	6,5,2	19	545
3	5,3,1	13	453
4	6,5,1	23	543
5	7,6,1	43	703
6	7,6,5,2,1	11	747
7	6,4,3,2,1	37	537
8	6,5,4	127	561
9	5,3,2	31	455
10	6,3,2	59	515
11	7,5,3	47	651
12	7,3,2	29	615
13	7,2,1	53	607
14	7,6,3,2,1	61	717
15	7,6,5,4,2	91	765



a) pedestal alone



b) peak alone

FIGURE 7: PEDESTAL SUBTRACTION PROCESS

3.0 R8 SIMULATION

In order to perform proper testing of the TIC performance, it was necessary to calculate the theoretical crosscorrelation function between two R8's. A software package, called XCORR, has been developed for this study to generate correlations and associated characteristics for the R8's. This program was written in the C programming language for 80386-based computers with a 80387 math coprocessor. This section will describe the program and the algorithms which the program implements. Also to be discussed are the assumptions made in the algorithms and limitations on the results of the program.

The program will perform ideal case correlation for the R8 class of m-sequences. The assumptions made in realizing this are as follows:

1. no noise or jamming;
2. no chip errors or data transitions within the correlation time;
3. perfect chip transition synchronization;
4. no sequence truncation or expansion; and
5. assume a perfect correlator, i.e., a correlator which does not introduce any noise or errors.

The XCORR program allows generation of either autocorrelation or crosscorrelation functions for the R8 class of m-sequences. The program is menu-driven and has the present capability of working with R8's only. The partial-period and full-period correlation functions can be generated for any portion of a sequence period, and for any starting position. Several of the correlation parameters can be varied and the results of these calculations can be displayed on high-resolution plots to either the screen, a plotter or a laser printer. The menus available in the program will now be described. The Main menu allows selection of a new pair of R8 sequences to correlate, the capability to change the correlation parameters and access to the Display Plots menu.

The correlation parameters which can be varied are:

1. initial conditions of the sequence generators which are configured in the Galois architecture;
2. integration window in number of chips which can be varied to correlate over any range of partial-period or full-period correlations;
3. relative phase shifts between the sequences; and
4. type of correlation either acousto-optic or digital.

The choices offered in the Display Plots menu are arranged so that many related plots can be analyzed with minimal menu switching. The functions available in the Display Plots menu are as follows:

1. Auto Increment Phase Shift by One Chip - allows viewing of the effects of stepping of the relative phase shift between two m-sequences;
2. Change Relative Phase Shift - allows setting of the relative phase shift between two m-sequences;
3. Auto Increment Integration Window by One Chip - allows viewing of the evolution of the degradation of the correlation function as the correlation time, (in units of chips), is modified by a small integer number of chips;
4. Change Integration Window - allows setting of the correlation time;
5. Compressed Screen Plot - allows screen display of the entire correlation function in high-resolution colour graphics;
6. Compressed Printer Plot - allows printing of the entire correlation function on one page using either a HP plotter or HP Laserjet printer;
7. Paged Screen Plot - sends a high-resolution display of the correlation function to the screen spread over four pages;
8. Paged Printer Plot - sends a high-resolution display of the correlation function to the printer or plotter spread over four pages;
9. Partial Period Statistics - generates the partial-period correlation magnitudes for a specific correlation start point for all relative phase shifts and determines the mean and variance of the correlation magnitude;
10. Return to Main Menu; and
11. Quit Program.

Note that the hard copy outputs from parts (6) and (8) can be sent to either the HP 7470A plotter or the HP Laserjet printer depending on the desired display format. The user has the option of sending the output immediately or generating a plot file and printing later in batch mode. A data file is also created when the printing is performed immediately. The data file which is created by XCORR is called Dwwxxyzz.DAT where

ww = first code identifier
 xx = second code identifier
 y = N for compressed full-period correlation plots
 = A,B,C,D for the four pages of a paged plot
 zz = relative phase shift (in hexadecimal) for
 full-period correlations
 = integration window (in hexadecimal) for
 partial-period correlations

The .DAT file generated by XCORR is used by LINPLOT to generate a .PLT file with the same filename as the .DAT file. For plotter outputs, LINPLOT routes the output to the plotter instead of the .PLT file. If a laser printer output is desired, then the .PLT file must be processed by the LASERPLOT software. LASERPLOT allows manipulation of magnification, line widths and many other parameters of a plot and outputs the plot to the laser printer. The option in XCORR to print immediately or later allows one to display a plot immediately or to batch process many plots at off-peak times.

The XCORR software was utilized to examine the autocorrelation and crosscorrelation functions for the R8's in order to predict the correlations which would be produced by the TIC. During the course of this investigation, features of the correlation functions were discovered which will be discussed later in this report. These features involved observation of patterns which linked decimation and crosscorrelation properties of m-sequences. As well, the concept of code families has been developed which describes the set of all m-sequence pairs which exhibit the same crosscorrelation functions under certain conditions. An examination of the effect of integrating over a partial period on the crosscorrelation function was also undertaken. This was performed in order to determine the effect of integration time window errors on the appearance of the crosscorrelation function, and in particular, the impact of these errors on the amplitude of the characteristic peaks which are used to classify a particular crosscorrelation function. Sample plots and figures concerning these features will also be presented later in this report.

4.0 ANALYSIS OF R8 CROSSCORRELATION PROPERTIES

The crosscorrelation functions have been generated using the XCORR software for all possible pairs of R8 m-sequences. It has been determined that techniques are available which significantly reduce the number of different crosscorrelation functions that need to be examined. Background material on decimation and correlation will now be given.

Let S denote an arbitrary m-sequence of period N , and consider the sequence T formed by taking every q^{th} bit of S . The sequence T is said to be the decimation by q of S and will be denoted by $S[q]$. Let $\text{gcd}(a,b)$ denote the greatest common divisor of the integers a and b . A decimation is termed proper if

$\gcd(q, N) = 1$, resulting in a sequence of period N . If T is generated by a proper decimation and S is an m -sequence, then T is also an m -sequence (although S and T may be the same). If $T = S[q]$ and $S = T[r]$, then q and r are termed inverse decimations. In other words, decimating sequence S by q and then by r will give back sequence S . q and r are inverse decimations if there exists some integer j , such that $qr = 2^j \bmod N$.

Two m -sequences T and U obtained by proper decimations q and r , respectively, of the same m -sequence S , are phase-shifted versions of the same m -sequence if q and r belong to the same cyclotomic coset [5]. In other words, if $\gcd(q, N) = 1$, $\gcd(r, N) = 1$ and $q = r \cdot 2^j \bmod N$ for some positive integer j . Note that the smallest member of the set $\{r \cdot 2^j \bmod N\}$ where $\gcd(r, N) = 1$ is termed the cyclotomic coset leader.

Given one m -sequence S of a given period, the remaining m -sequences of the same period can be obtained from S by decimating S by all of the proper decimations. These correspond to all of the cyclotomic coset leaders for the Galois field $GF(N)$. As an example, Table 1 shows the set of all m -sequence characteristic polynomials for the $R8$'s and their corresponding proper decimations.

The relationship between m -sequences and their decimations is summarized using decimation relations [3]. On a decimation relation graph, the decimations required to generate one sequence from another are detailed. An example for the $R5$'s [3] is given in Figure 8 which consists of six sequences. Each side of the hexagon corresponds to a decimation by 3 if traversed clockwise and to a decimation by 11 if traversed counterclockwise. The dashed lines correspond to decimation by 5 if traversed clockwise and to decimation by 7 if traversed counterclockwise. Finally, traversing a diameter corresponds to decimation by 15. These decimation relations are important because they demonstrate graphically that knowledge of one sequence gives complete knowledge of all of the possible m -sequences of the same period including the characteristic polynomial. The decimation relation graph for the $R8$'s is shown in Figure 9 [3].

The decimation properties of m -sequences can be exploited with respect to the crosscorrelation function. The full-period crosscorrelation function between two m -sequences is the same for all m -sequences of the same period which are related by the same decimation [4]. Hence, to characterize all possible crosscorrelating functions requires only calculating a number of crosscorrelation functions equal to the number of proper cyclotomic cosets. It should be emphasized that the interest in this note is in the crosscorrelation spectrum, i.e., the set of values taken on by the crosscorrelation function and the number of occurrences of each value. Further discussions of the effect of decimation and relative phase shifts on the crosscorrelation function can be found in [5].

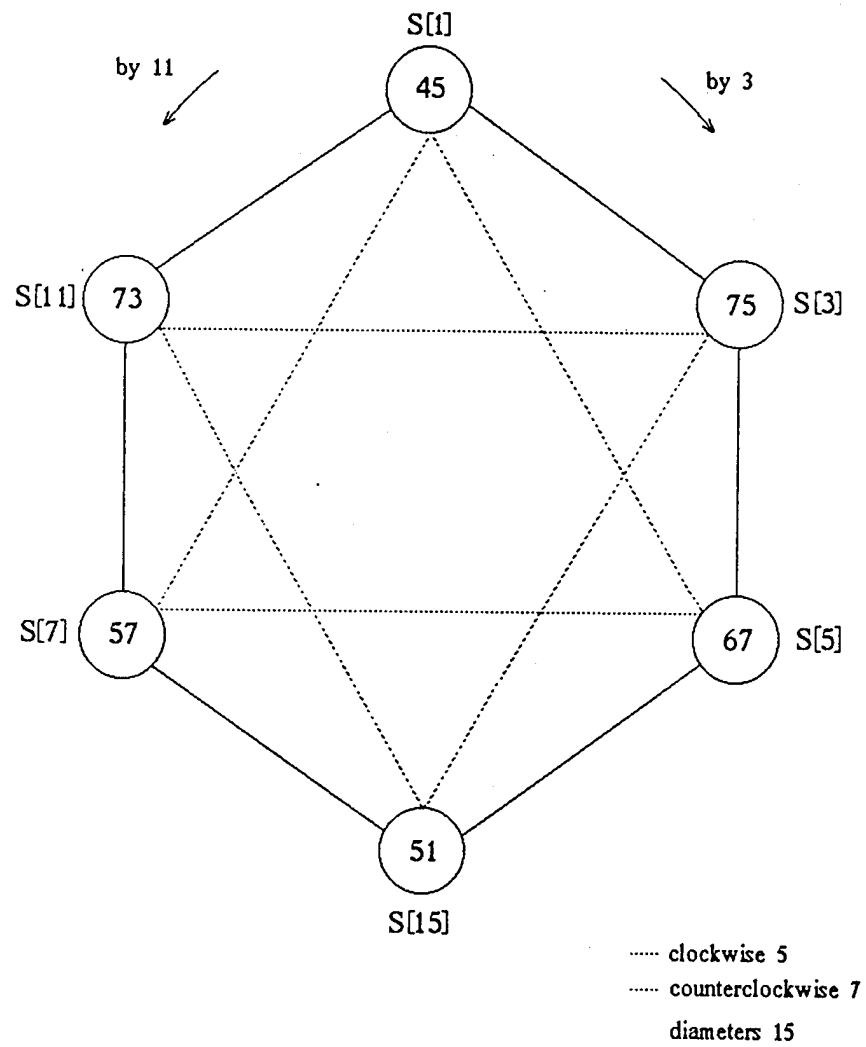


FIGURE 8: DECIMATION RELATIONS FOR THE R5'S (FROM [5])

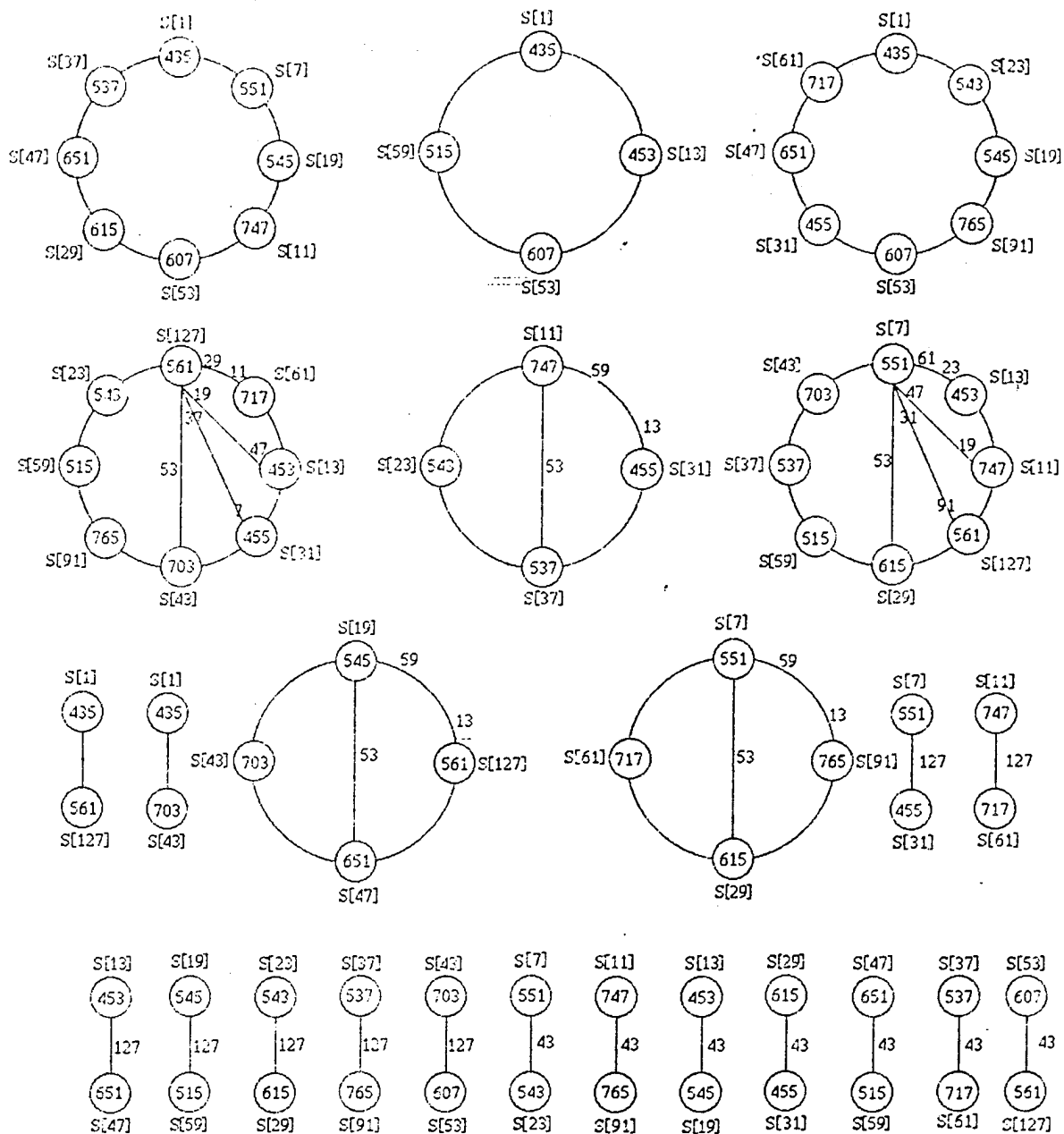


FIGURE 9: DECIMATION RELATIONS FOR THE R8'S (FROM [5])

R8 Code Families

# 1:	1 [1]	254(-1)	1(255)				
# 2:	7 [37]	16(-33)	52(-17)	104(-1)	68(15)	14(31)	1(63)
# 3:	11 [29]	1(-65)	8(-33)	64(-17)	100(-1)	68(15)	10(31)
	4(47)						
# 4:	13 [59]	18(-33)	48(-17)	100(-1)	84(15)	4(47)	1(63)
# 5:	19 [47]	88(-17)	87(-1)	64(15)	8(31)	8(47)	
# 6:	23 [61]	88(-17)	89(-1)	56(15)	20(31)	2(63)	
# 7:	31 [91]	80(-17)	119(-1)	16(15)	40(31)		
# 8:	43 [43]	8(-33)	60(-17)	108(-1)	76(15)	1(63)	2(95)
# 9:	53 [53]	96(-17)	59(-1)	96(15)	4(63)		
#10:	127 [127]	8(-29)	16(-25)	8(-21)	18(-17)	24(-13)	16(-9)
	32(-5)	16(-1)	16(3)	20(7)	16(11)	16(15)	
	16(19)	20(23)	8(27)	5(31)			

FIGURE 10: CODE FAMILIES FOR THE R8'S (FROM [5])

If two proper decimations q and r are inverse decimations, then the crosscorrelation spectrum which results will be the same for both decimation by q and for decimation by r . The set of all sequence pairs which satisfy a given decimation and its inverse will be termed an inverse pair group and will be described by the inverse decimation pair and its corresponding crosscorrelation spectrum. The set of all inverse pair groups which have the same crosscorrelation spectrum is called a code family, i.e., the number of code families equals the number of unique crosscorrelation spectra for a given R_n .

The code families for the R8's are shown in Figure 10. Figure 10 is formatted such that the inverse decimation pairs are given as $a_1[b_1]$, $a_2[b_2]$, ... with the corresponding weight distribution given in the form $x_1(y_1)$, $x_2(y_2)$... The x_i values correspond to the number of occurrences of the crosscorrelation magnitudes y_i . Thus, for the R8 inverse decimation pair 1[1] (corresponding to an autocorrelation), the weight distribution is 254 occurrences of -1 and 1 occurrence of 255. It is interesting to note that the code families for the R8's have only one inverse pair group each. Corresponding to each of the code families from Figure 10, the characteristic crosscorrelation functions are shown in Figures 11 to 13. It is observed that each of the crosscorrelation functions have distinctive features which allow each to be distinguishable from any other. For example, the crosscorrelation function of family #8 has two correlation peaks of magnitude 95 and a secondary peak of magnitude 63.

4.1 Partial-Period CrossCorrelation Properties for the R8's

Partial-period crosscorrelation functions are produced when the integration time of the detector array is not an exact multiple of the code length. The crosscorrelation is then the result of a correlation over a window containing a number of chips smaller than the period of the code (255 chips for a R8). The particular features of each partial-period crosscorrelation function depends on the integration time, the relative phase shift between the two codes and the starting point of the integration. For an R8, the number of integrated chips can vary between 1 and 254, 255 different relative phase shifts are possible and 255 starting points are possible. As there are $16 \times 15 = 240$ possible full-period crosscorrelation functions for the R8's, a total of

$$16 \times 15 \times 254 \times 255 \times 255 = 3,963,924,000$$

different partial-period crosscorrelation functions are possible.

However, it has been demonstrated in the previous sections that the full-period crosscorrelation functions can be regrouped into 9 families. It is reasonable that a partial-period crosscorrelation function produced by integrating a number of chips close to 255 will not be that different from a full-period correlation. As the number of chips integrated diminishes, the similarity between the partial-period correlation

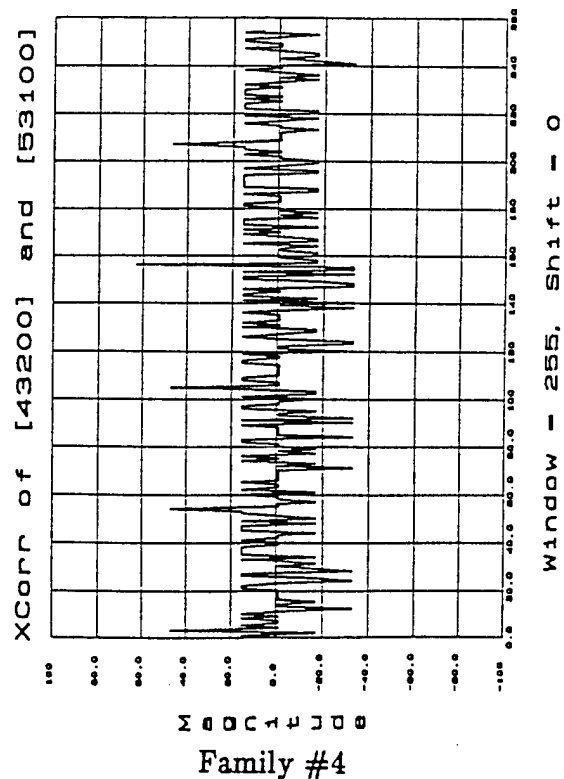
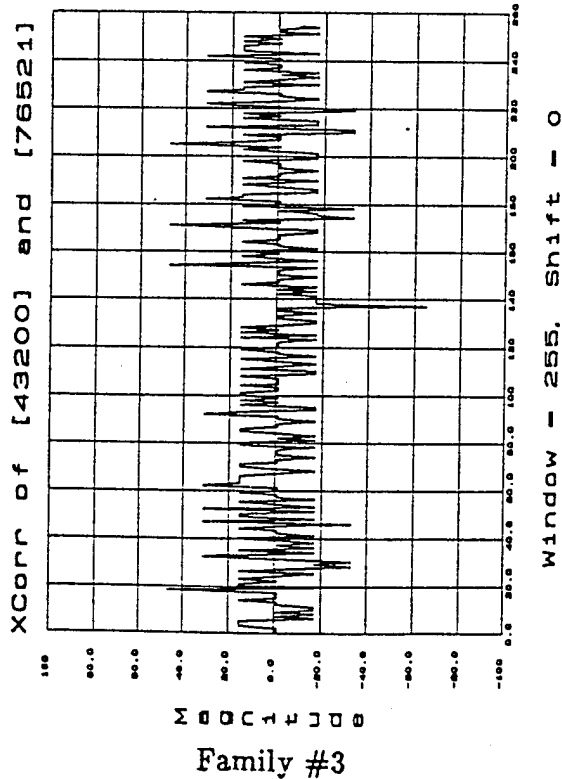
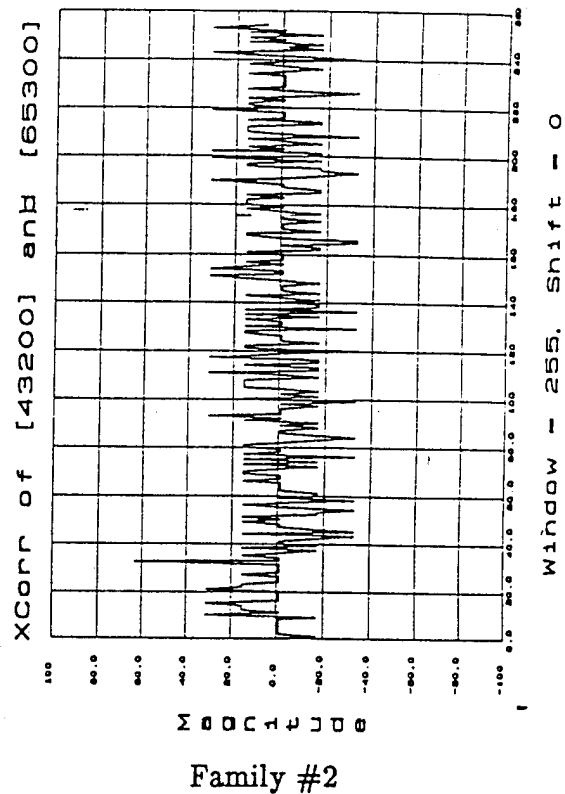
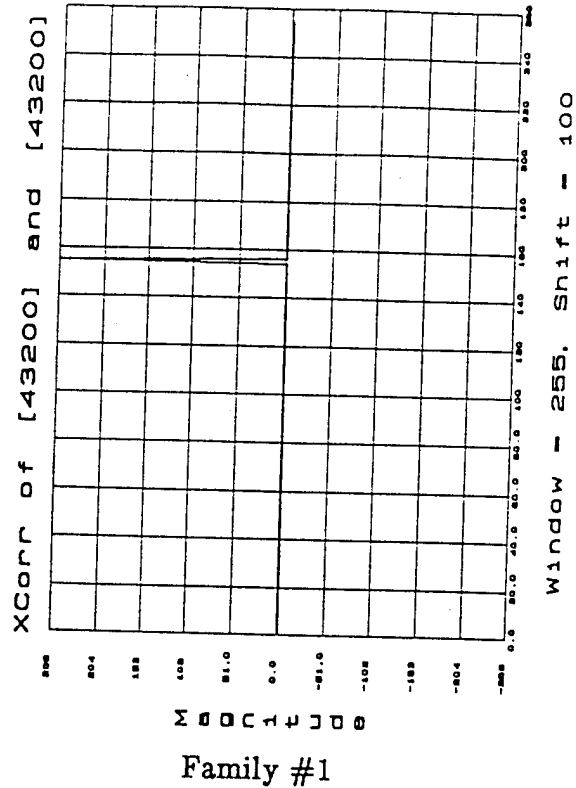


FIGURE 11: CROSSCORRELATION FUNCTIONS FOR THE R8'S
(FROM [5]) (1)

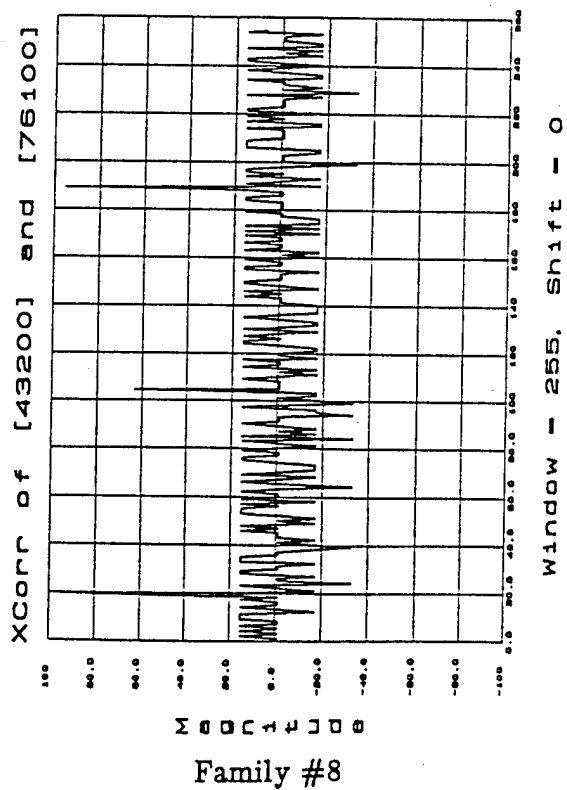
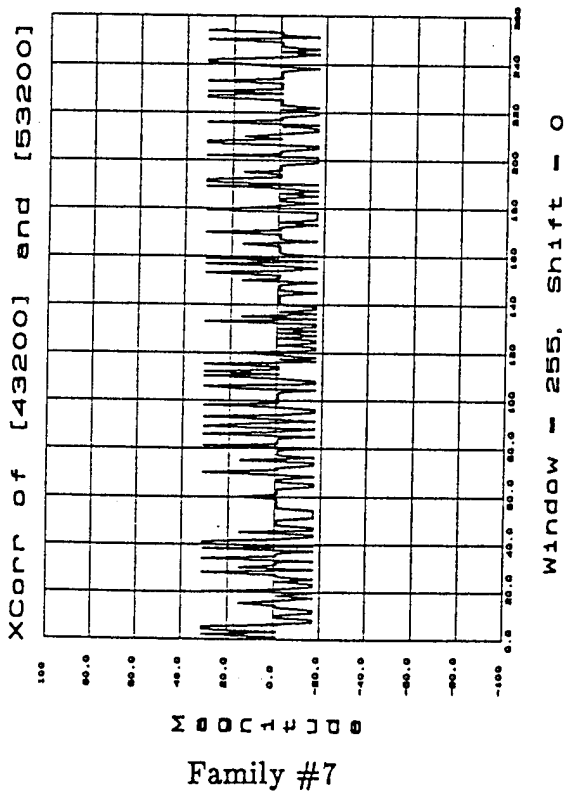
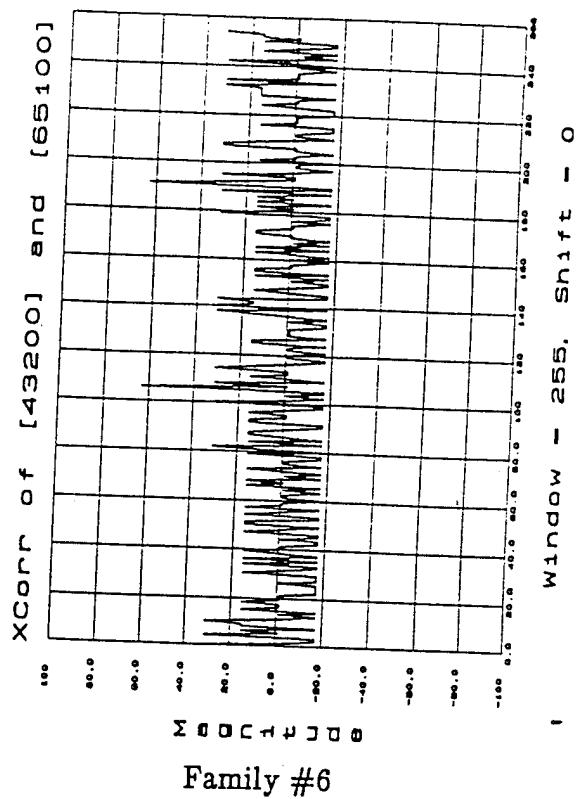
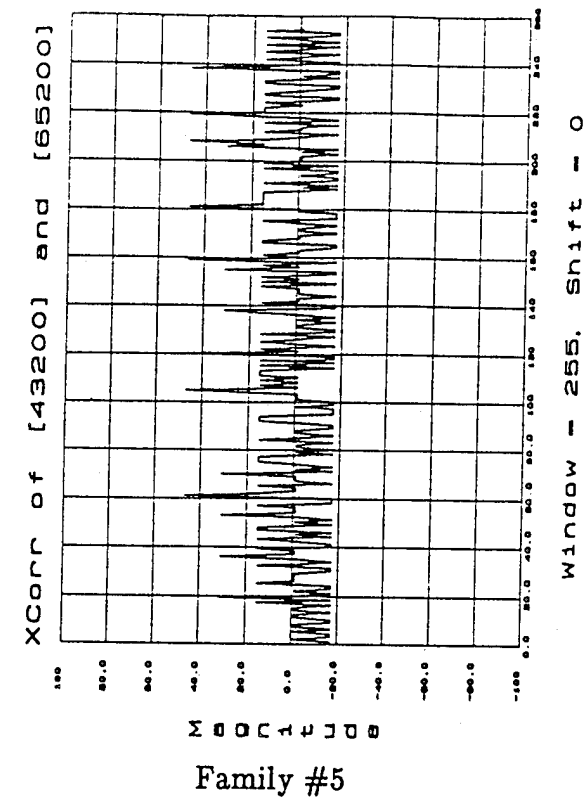


FIGURE 12: CROSSCORRELATION FUNCTIONS FOR THE R8'S
(FROM [5]) (2)

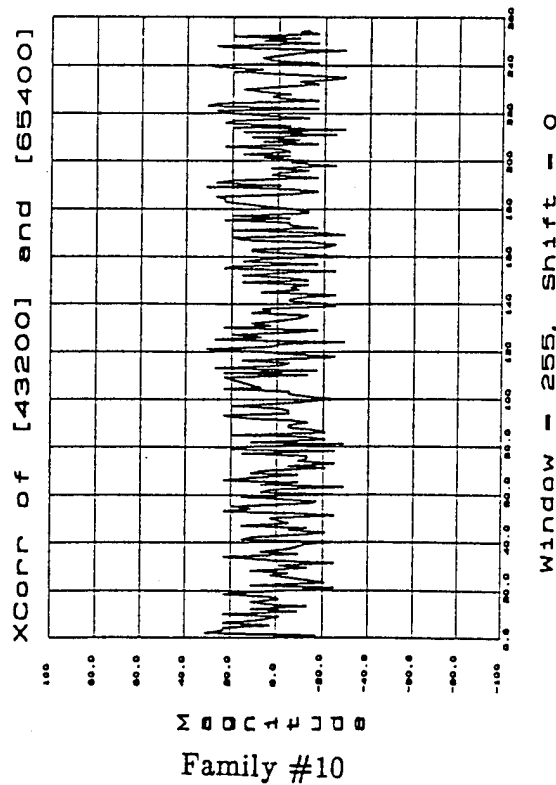
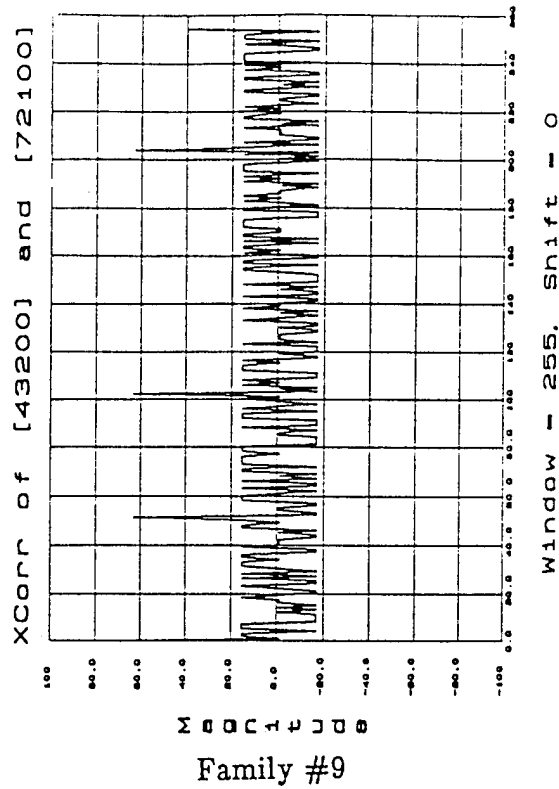


FIGURE 13: CROSSCORRELATION FUNCTIONS FOR THE R8'S
(FROM [5]) (3)

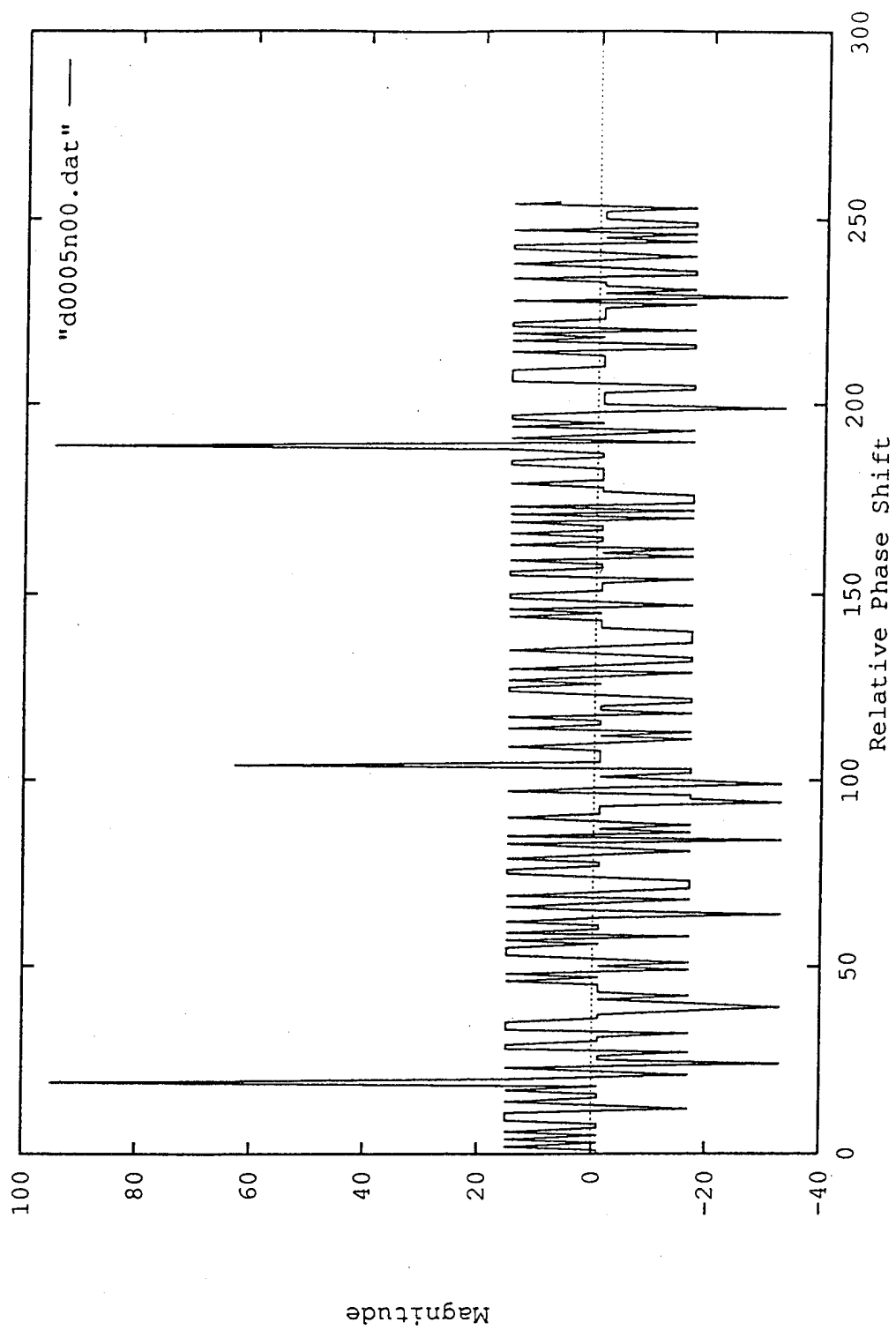


FIGURE 14: CROSSCORRELATION FUNCTIONS FOR CODES 0 AND 5

and the full-period correlation should disappear. It is also expected that somewhat different partial-period crosscorrelation patterns will be produced by the 255 possible phase shifts of the codes for each particular integration window investigated.

A limited study of the partial-period crosscorrelation function between codes 0 and 5 of Table 1 was made to provide insight into their properties. The full-period crosscorrelation between codes 0 and 5 is characterized by the presence of two very strong peaks with an amplitude of 95 and one strong peak with an amplitude of 63, as seen in Figure 14. Many other peaks are present between the amplitudes of -33 and 15. A member of this family was selected because it is believed that codes 0 and 5 give the type of full-period crosscorrelation function whose features are the easiest to identify and detect in the presence of noise. Three windows with integration times of 250, 230 and 210 chips were considered in order to follow the evolution of the partial-period crosscorrelation function as the integration is performed on a decreasing number of chips. Figures 15 to 17 respectively show the amplitude of the primary, secondary and tertiary peaks as a function of the phase shift for windows of 250 chips, 230 chips and 210 chips. All possible phase shifts were considered for each of the three partial windows and the starting point of the integration was always the same. The amplitude of the peak is seen to fluctuate around a mean value with some variance. These values are seen in Table 2. The average values of the peaks is seen to decrease and the variance increases as the size of the partial integrating window decreases. It is also clear from Figure 17 that the utilization of a partial integration window that is only 20% smaller than the full period window is enough to make the identification of the features of the crosscorrelation function difficult.

TABLE 2: MEAN AND VARIANCE OF THE THREE HIGHEST PEAKS OF THE PARTIAL-PERIOD CROSSCORRELATION FUNCTION BETWEEN CODES 0 AND 5 FOR DIFFERENT INTEGRATION TIME WINDOWS

	Integration Window					
	T = 250		T = 230		T = 210	
	Mean	Var	Mean	Var	Mean	Var
Peak 1 at 95	93.1	2.8	85.7	11.1	78.2	19.5
Peak 2 at 63	61.8	3.9	56.8	17.2	51.9	19.5
Peak 3 at 95	93.1	3.6	85.7	12.9	78.2	19.7

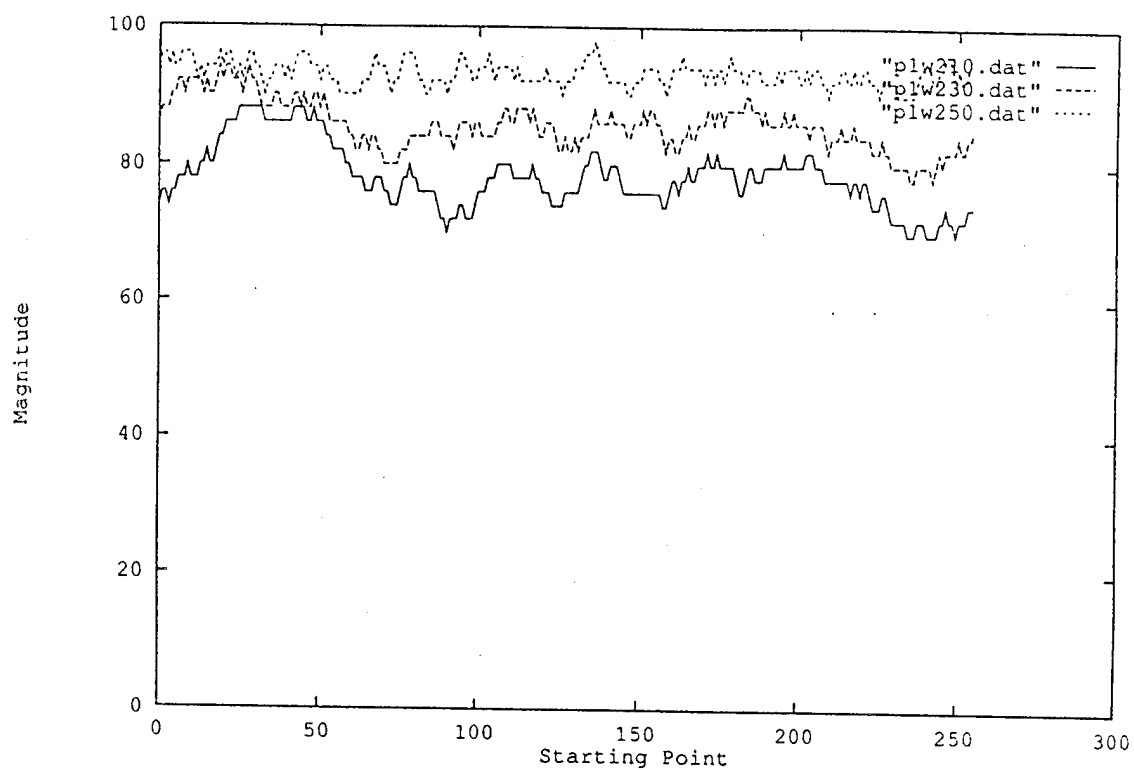


FIGURE 15: VARIATION IN PEAK AMPLITUDES FOR THE PARTIAL-PERIOD CROSSCORRELATION BETWEEN CODES 0 AND 5; PEAK 1 AT 95, INTEGRATION OF 250, 230 AND 210 CHIPS

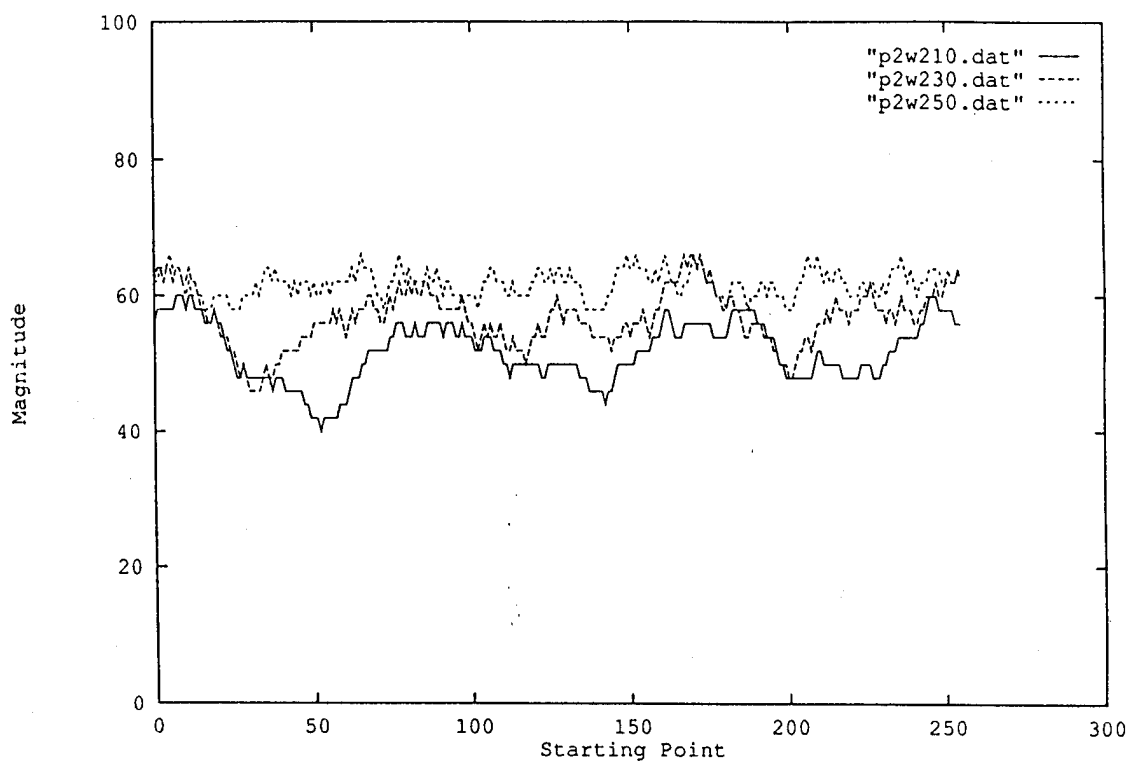


FIGURE 16: VARIATION IN PEAK AMPLITUDES FOR THE PARTIAL-PERIOD CROSSCORRELATION BETWEEN CODES 0 AND 5; PEAK 2 AT 63, INTEGRATION OF 250, 230 AND 210 CHIPS

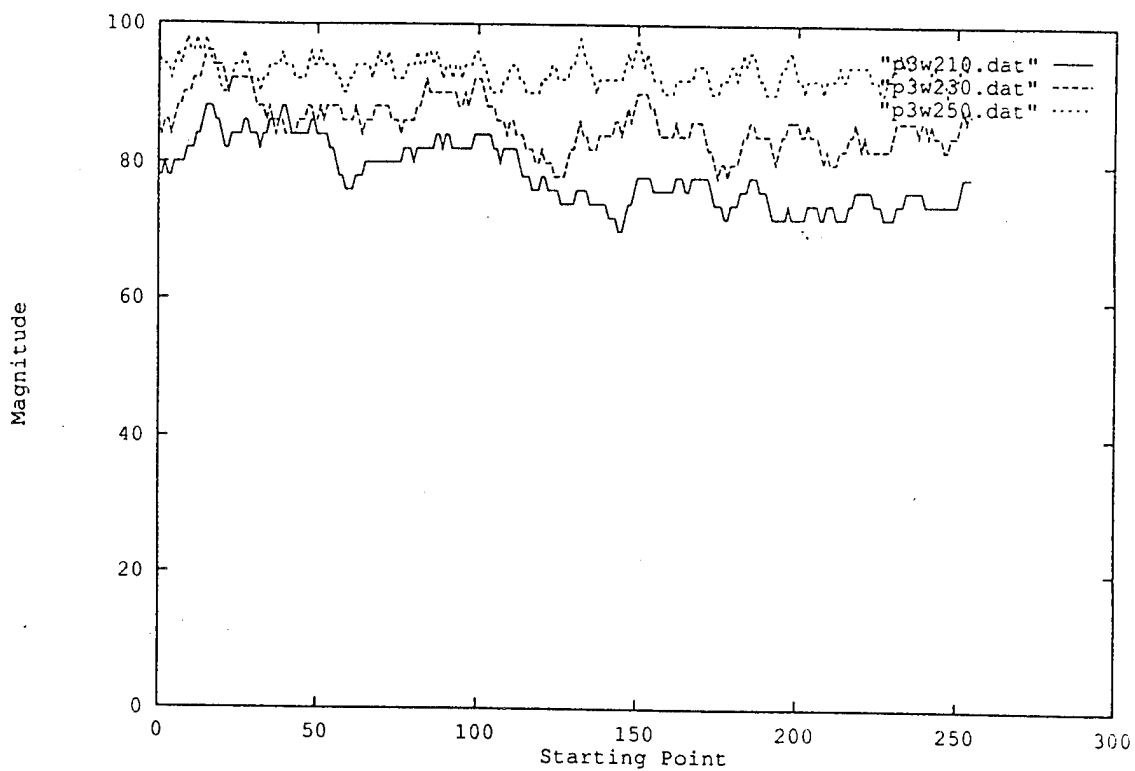


FIGURE 17: VARIATION IN PEAK AMPLITUDES FOR THE PARTIAL-PERIOD CROSSCORRELATION BETWEEN CODES 0 AND 5; PEAK 3 AT 95, INTEGRATION OF 250, 230 AND 210 CHIPS

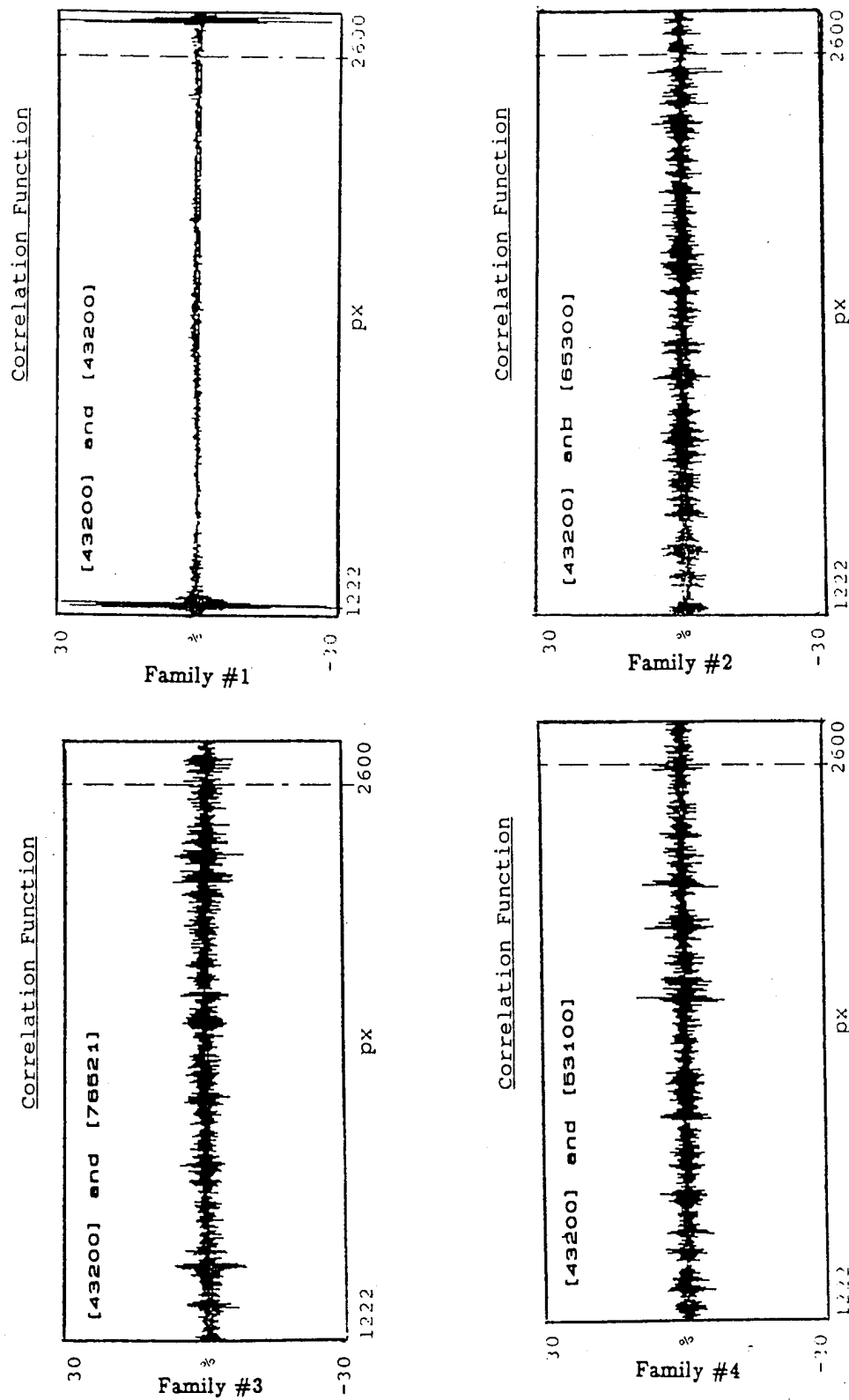


FIGURE 18: OPTICALLY PRODUCED CROSSCORRELATIONS FUNCTIONS FOR THE R8'S (1)

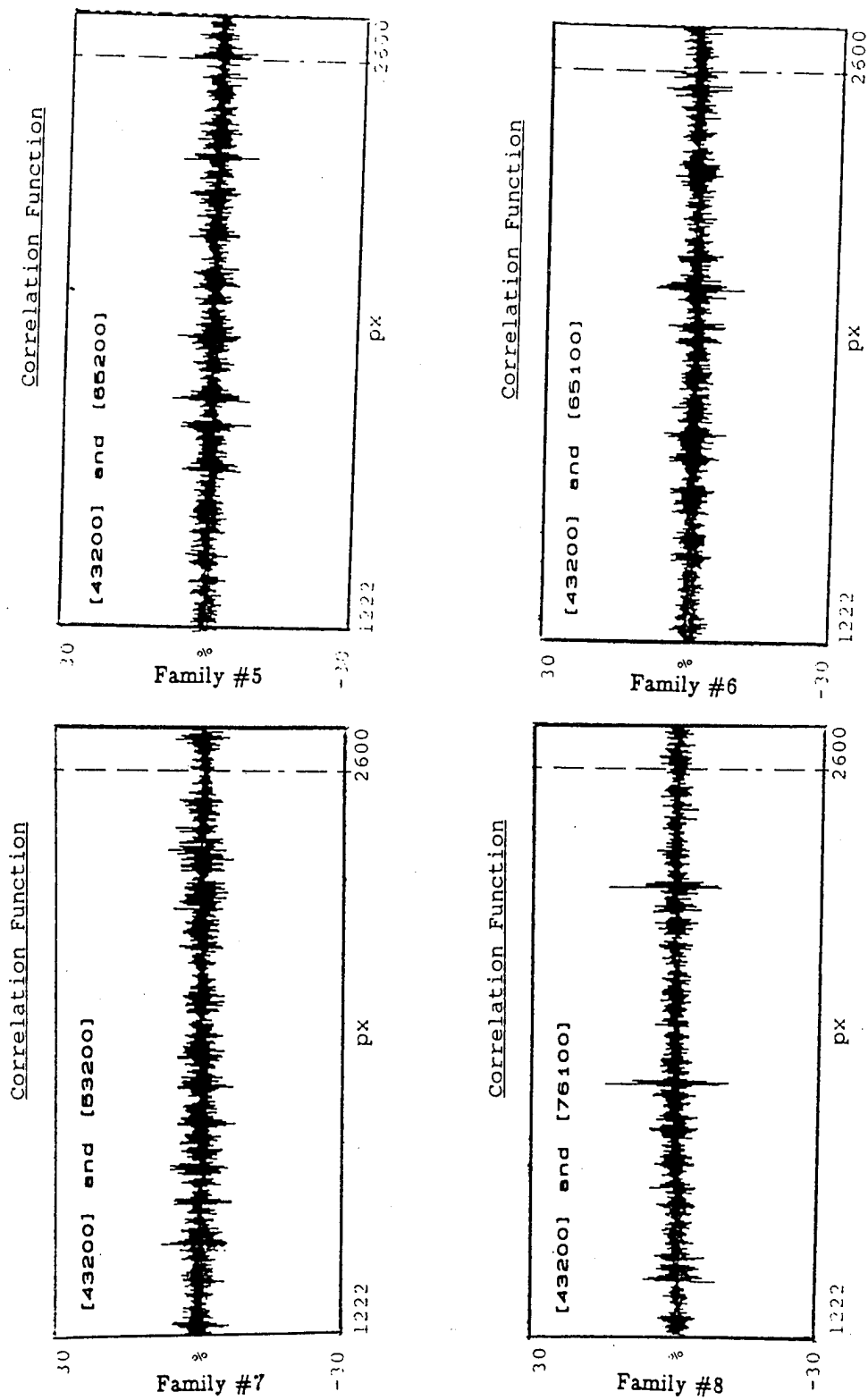


FIGURE 19: OPTICALLY PRODUCED CROSSCORRELATIONS FUNCTIONS FOR THE R8'S (2)

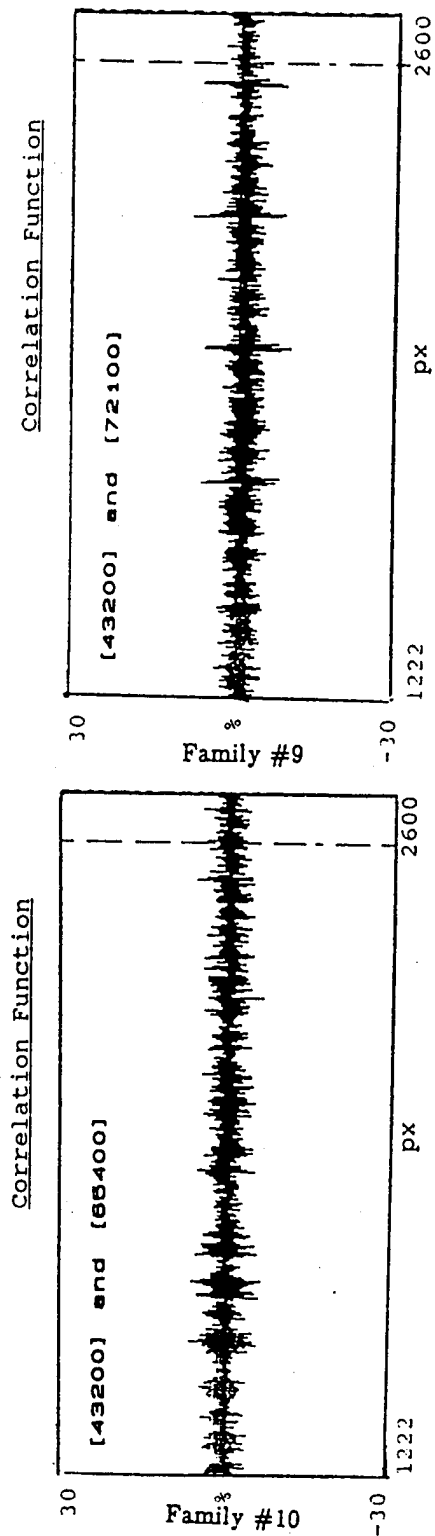


FIGURE 20: OPTICALLY PRODUCED CROSSCORRELATIONS
FUNCTIONS FOR THE R8'S (3)

5.0 EXPERIMENTAL RESULTS

The TIC described in Section 2.0 was used to calculate the full-period crosscorrelations of each of the nine families of the R8's. The 10th family is the autocorrelation. The experimental results are illustrated in Figures 18, 19 and 20 and they can be compared to the theoretical results illustrated in Figures 11, 12 and 13.

Both experimental and theoretical results illustrate full period crosscorrelations. However, the initial fill of the shift-register generating the sequences is not the same for the experimental and theoretical results so the relative positions of the partial correlation peaks are not expected to be the same, although the number of peaks with a certain height is the same. Table 3 contains a list of the salient features of the crosscorrelations for the families of R8's. The crosscorrelations having the most recognizable features are listed first. The families that exhibit no easily distinguishable feature have no entry in Table 3.

TABLE 3: FEATURES OF THE CROSSCORRELATION FUNCTIONS FOR THE R8'S

FAMILY #	HEIGHT OF THE TALLEST PEAK	# OF TALLEST PEAK	HEIGHT OF THE SECOND TALLEST PEAK	# OF SECOND TALLEST PEAK
1	255	1		
8	95	2	63	1
9	63	4		
6	63	2		
2	63	1		
4	63	1	47	4
3	63	1		
5	47	8		
7				
10				

Family #1 illustrates the particular case of the autocorrelation of two R8s and has the most easily recognizable features of all patterns. One can notice the very low level of noise, between the correlation peaks of the optically calculated correlation (see Figure 18). One can also notice that the segment of autocorrelation illustrated in Figure 18 is longer than the length of the sequence (255 chips) being correlated. The display of a second correlation peak 255 chips away from the first peak results because the autocorrelation, like the sequence

itself, has a period of 255 chips. The comparison of the other experimental results with theoretical results indicate that the crosscorrelation of family 8 and 9 could be visually identified. The other optical crosscorrelations cannot be visually identified. Artificial neural networks have been proposed [6] to perform such identification. Improved performance may result.

6.0 CONCLUSION

The software developed to study the crosscorrelation properties of R8's is presented together with an analysis of their partial-period crosscorrelations. The operation and the main features of the optical correlator used to calculate experimentally the crosscorrelations are presented. The comparison of the experimental with the theoretical results shows that it is possible to identify from the optical results the families whose crosscorrelation have the strongest features.

7.0 REFERENCES

- [1] M.W. Casseday, N.J. Berg, I.J. Abramovitz and J.N. Lee, "Wide-Band Signal Processing Using the Two-Beam Surface Acoustic Wave Acousto-Optic Time Integrating Correlator", IEEE Transactions on Sonics and Ultrasonics, Vol. SV-28, No. 3, pp. 205-212, May 1981.
- [2] N. Brousseau and J.W.A. Salt, "Analysis and Optimization of the Data Collection Process of Time-Integrating Correlators", DREO TN 95-5.
- [3] D.V. Sarwate and M.B. Pursley, "Crosscorrelation Properties of Pseudorandom and Related Sequences", Proc. IEEE, Vol. 68, No. 5, pp 593-619, May 1980.
- [4] H.M. Trachtenberg, "On the Crosscorrelation Functions of Maximal Linear Recurring Sequences", PhD Dissertation, Dept of Electrical Engineering, University of Southern California, Los Angeles, CA, Jul 1970.
- [5] S.A. Faulkner, "Interception of Direct-Sequence Spread Spectrum Codes by Weight Distribution Analysis", MEng Thesis, Dept of Electronics, Carleton University, Ottawa, Ontario, 1989.
- [6] J.W. DeBarry and D.M. Norman, "Classification of Acousto-Optic Correlation Signatures of Spread-Spectrum Signals Using Artificial Neural Networks", Air Force Institute of Technology (AU) Report 89-D-10.

SECURITY CLASSIFICATION OF FORM
(highest classification of Title, Abstract, Keywords)

DOCUMENT CONTROL DATA

(Security classification of title, body of abstract and indexing annotation must be entered when the overall document is classified)

1. ORIGINATOR (the name and address of the organization preparing the document. Organizations for whom the document was prepared, e.g. Establishment sponsoring a contractor's report, or tasking agency, are entered in section 8.) DEFENCE RESEARCH ESTABLISHMENT OTTAWA NATIONAL DEFENCE SHIRLEYS BAY, OTTAWA, ONTARIO K1A 0Z4 CANADA		2. SECURITY CLASSIFICATION (overall security classification of the document including special warning terms if applicable) UNCLASSIFIED	
3. TITLE (the complete document title as indicated on the title page. Its classification should be indicated by the appropriate abbreviation (S,C or U) in parentheses after the title.) STUDY OF THE CROSS-CORRELATION PROPERTIES OF THE 8-STAGE MAXIMAL LENGTH SEQUENCES FOR THE TESTING OF A TIME-INTEGRATING CORRELATOR (U)			
4. AUTHORS (Last name, first name, middle initial) FAULKNER, S. AND BROUSSEAU, N.			
5. DATE OF PUBLICATION (month and year of publication of document) SEPTEMBER 1995		6a. NO. OF PAGES (total containing information. Include Annexes, Appendices, etc.) 33	6b. NO. OF REFS (total cited in document) 6
7. DESCRIPTIVE NOTES (the category of the document, e.g. technical report, technical note or memorandum. If appropriate, enter the type of report, e.g. interim, progress, summary, annual or final. Give the inclusive dates when a specific reporting period is covered.) DREO TECHNICAL NOTE			
8. SPONSORING ACTIVITY (the name of the department project office or laboratory sponsoring the research and development. Include the address.) DEFENCE RESEARCH ESTABLISHMENT OTTAWA NATIONAL DEFENCE SHIRLEYS BAY, OTTAWA, ONTARIO K1A 0Z4 CANADA			
9a. PROJECT OR GRANT NO. (if appropriate, the applicable research and development project or grant number under which the document was written. Please specify whether project or grant) 02J01		9b. CONTRACT NO. (if appropriate, the applicable number under which the document was written)	
10a. ORIGINATOR'S DOCUMENT NUMBER (the official document number by which the document is identified by the originating activity. This number must be unique to this document.) DREO TECHNICAL NOTE 95-9		10b. OTHER DOCUMENT NOS. (Any other numbers which may be assigned this document either by the originator or by the sponsor)	
11. DOCUMENT AVAILABILITY (any limitations on further dissemination of the document, other than those imposed by security classification) <input checked="" type="checkbox"/> Unlimited distribution <input type="checkbox"/> Distribution limited to defence departments and defence contractors; further distribution only as approved <input type="checkbox"/> Distribution limited to defence departments and Canadian defence contractors; further distribution only as approved <input type="checkbox"/> Distribution limited to government departments and agencies; further distribution only as approved <input type="checkbox"/> Distribution limited to defence departments; further distribution only as approved <input type="checkbox"/> Other (please specify):			
12. DOCUMENT ANNOUNCEMENT (any limitation to the bibliographic announcement of this document. This will normally correspond to the Document Availability (11). However, where further distribution (beyond the audience specified in 11) is possible, a wider announcement audience may be selected.)			

UNCLASSIFIED

SECURITY CLASSIFICATION OF FORM

DCD03 2/06/87

UNCLASSIFIED

SECURITY CLASSIFICATION OF FORM

13. ABSTRACT (a brief and factual summary of the document. It may also appear elsewhere in the body of the document itself. It is highly desirable that the abstract of classified documents be unclassified. Each paragraph of the abstract shall begin with an indication of the security classification of the information in the paragraph (unless the document itself is unclassified) represented as (S), (C), or (U). It is not necessary to include here abstracts in both official languages unless the text is bilingual).

(U) The purpose of this DREO Technical Note is to present experimental and theoretical results on the properties of the cross correlations of maximum length direct sequences (m-sequences). The code correlation families and the relationship between full-period and partial-period correlations are described. Results from the software developed to study the cross-correlation properties of the 8-stage m-sequences, denoted R8's, as well as, results obtained from the optical correlator and the theoretical studies are presented. The software developed to analyze the cross-correlation functions was also suitable for the study of partial-period correlation functions and the effects of phase shifts on partial-period correlation functions. Properties of partial-period correlation functions are also analyzed and a generalization to longer m-sequences is presented. The results from the optical correlator demonstrate that it is possible to visually identify the m-sequences family associated with the cross-correlations for those which have the strongest features.

14. KEYWORDS, DESCRIPTORS or IDENTIFIERS (technically meaningful terms or short phrases that characterize a document and could be helpful in cataloguing the document. They should be selected so that no security classification is required. Identifiers, such as equipment model designation, trade name, military project code name, geographic location may also be included. If possible keywords should be selected from a published thesaurus. e.g. Thesaurus of Engineering and Scientific Terms (TEST) and that thesaurus-identified. If it is not possible to select indexing terms which are Unclassified, the classification of each should be indicated as with the title.)

TIME-INTEGRATING CORRELATOR
PARTIAL PERIOD CORRELATION OF DIRECT SEQUENCES
OPTICAL CORRELATION
CROSS-CORRELATION OF DIRECT SEQUENCES

UNCLASSIFIED

SECURITY CLASSIFICATION OF FORM